

Variation of Laser Energy Transfer Efficiency with Weld Pool Depth

Phillip W. Fuerschbach
 Danny O. MacCallum
 Sandia National Laboratories
 Albuquerque, New Mexico 87185-0340

RECEIVED

NOV 17 1995

OSTI

Abstract

A series of CO₂ laser welds were made at a constant beam irradiance of 6 MW/cm² on 304 stainless steel with travel speeds selected to produce welds with varying levels of weld penetration. Using a Seebeck envelope calorimeter, the net heat input to the part was measured for each weld. It was found that the energy transfer efficiencies varied from 0.29 to 0.86, and decreased at high travel speeds where the weld penetration depth was as shallow as 0.13 mm. The decrease in beam absorption with decreasing weld pool depth is consistent with an absorption mechanism that requires multiple internal reflections within the weld pool. Equations have been developed which connect the keyhole cavity dimensions with the energy transfer efficiency, and correlations with the experimental data have determined the keyhole cavity radius to be 0.1 mm for a focused laser beam with a spot radius of 0.059 mm.

Introduction

For laser beam welding at powers less than 2000 watts, it is known that both weld penetration depth and beam absorption increase as the laser beam irradiance increases. What is unclear, is whether enhanced laser beam absorption (as high as 90%) requires a high irradiance. Several complex absorption mechanisms have been proposed for laser welding, which may be disregarded, if the weld pool shape is found to be the primary contributor to absorption.

Work by Huntington and Eagar (Ref. 1) demonstrated an important correlation between the weld joint geometry and absorption of the laser beam. More recent work by Kim et al (Ref. 2) clearly indicates an increase in energy transfer efficiency as the weld pool depth increases. But in calorimetry by Fuerschbach (Ref. 3) energy transfer efficiencies of 90% were found for weld pool depths that ranged from as little as 0.9 mm to 2.7 mm. The work concluded that variations in travel speed do not seem to affect coupling. Only when beam irradiance was reduced was the energy transfer efficiency seen to decrease. Moreover, no correlation could be found between the fusion zone aspect ratio and the energy transfer efficiency.

Is coupling at high irradiance improved because of the onset of an intensity driven absorption mechanism, or more simply because of the development of a weld pool geometry that permits multiple internal reflections of the laser beam?

To help answer this question experimentally, it is necessary to make welds at a high laser beam irradiance that do not permit multiple internal reflections within the weld pool. To corroborate and extend the work by Kim et al (Ref. 2), it was the goal of this study to make high irradiance laser welds at extremely high travel speeds and thereby create shallow weld pools.

Experimental

Single pass CO₂ laser welds were made at 6 MW/cm² on 304 stainless steel round plates. The travel speeds were selected to produce welds with varying levels of weld penetration. In order to produce shallow welds at this high irradiance, very fast welds were required. The plate dimensions were 12.7 mm thick by 102 mm diameter with a machined surface. The plates were spun under the laser beam on a rotary fixture in order to obtain the high travel speeds required. Ten welds were made; two replicates for each of the five travel speeds. The five levels of travel speed were: 106, 212, 318, 424, and 530 mm/s. The welds were made on a Photon Sources V1200 slow axial flow CO₂ laser operating in the continuous wave mode. Laser output power was 930 watts. The laser beam was focused with a 2.5 in focal length aspheric ZnSe lens. The spotsize with this lens and laser has been previously measured to be 0.118 mm.

Using a Seebeck envelope calorimeter, the net heat input to the part was measured for each weld. The test specimens were welded on the rotary fixture and immediately placed in the calorimeter after welding. The calorimeter walls were maintained at room temperature with a constant temperature bath. The calorimeter operates on the gradient layer principle (Ref. 4) and produces a voltage output that is proportional to the flux through the walls during the time required for the weld sample to cool to room temperature. For short duration weld times, the energy losses with this experimental technique due to radiation, convection, and evaporation are thought to be 1% or less of the measured energy (Ref. 5). The calorimeter has been shown to produce a very linear response for different closure time durations and heat input levels. The output voltage versus time trace was recorded on a digital storage oscilloscope, then integrated to determine the energy in joules absorbed by the workpiece during the weld. The reported values of energy transfer efficiency (η_t) were calculated by dividing the net heat input (Q_i) by the laser output energy (Q_o), which is the output power multiplied by the shutter open time.

$$\eta_t = \frac{Q_i}{Q_o} \quad [1]$$

Results and Discussion

The expected decrease in measured weld penetration with increasing travel speed is shown in Figure 1. The decrease in penetration is due to a reduction in the local amount of energy available for melting as the travel speed was increased. Certainly if the travel speed is increased sufficiently there will be no melting of the base metal. The experimental goal of obtaining welds at the same beam irradiance with varying degrees of penetration was achieved in this manner. Figure 2 shows a sample metallographic cross-section of a weld and illustrates the geometry that is widely considered to be representative of keyhole mode welding.

The correlation between energy transfer efficiency and weld penetration is shown in Figure 3. One can see that for the shallow welds only a small fraction of the incident laser beam energy is absorbed by the workpiece, but when the weld penetration approaches a depth of 1 mm, a much higher fraction of the incident energy is absorbed. This decrease in energy transfer efficiency as penetration decreases agrees with the work of Kim et al. (Ref. 2) Comparison of the results of these two studies however indicates that this dependence is very application specific.

This decrease in beam absorption with decreasing weld pool depth is consistent with an absorption mechanism that requires multiple internal reflections within the weld pool—as the weld penetration depth becomes more shallow, the incident light rays are more readily reflected out of the weld pool cavity. The theory of multiple internal

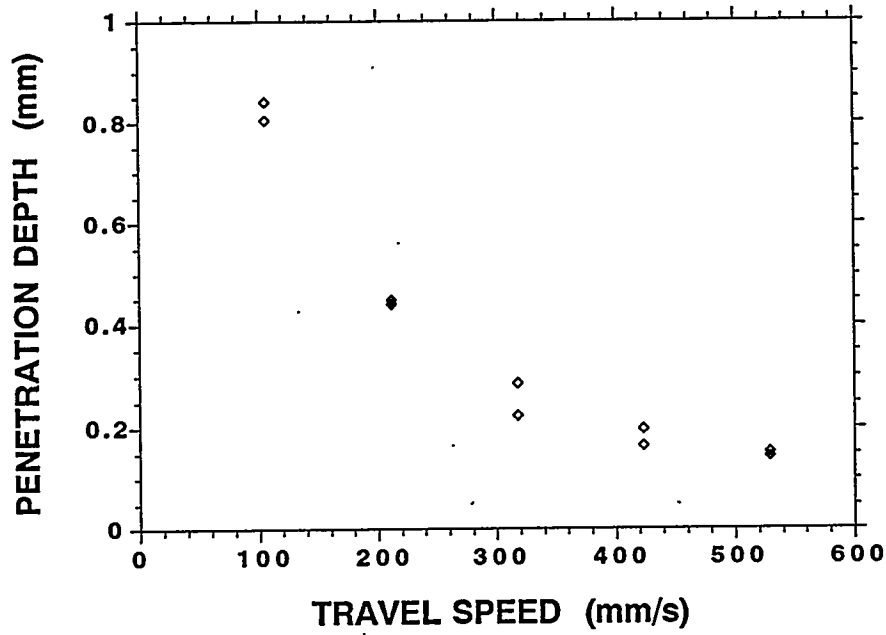


Fig. 1—Effect of travel speed on weld penetration for a constant beam irradiance: 9.1 MW/cm².

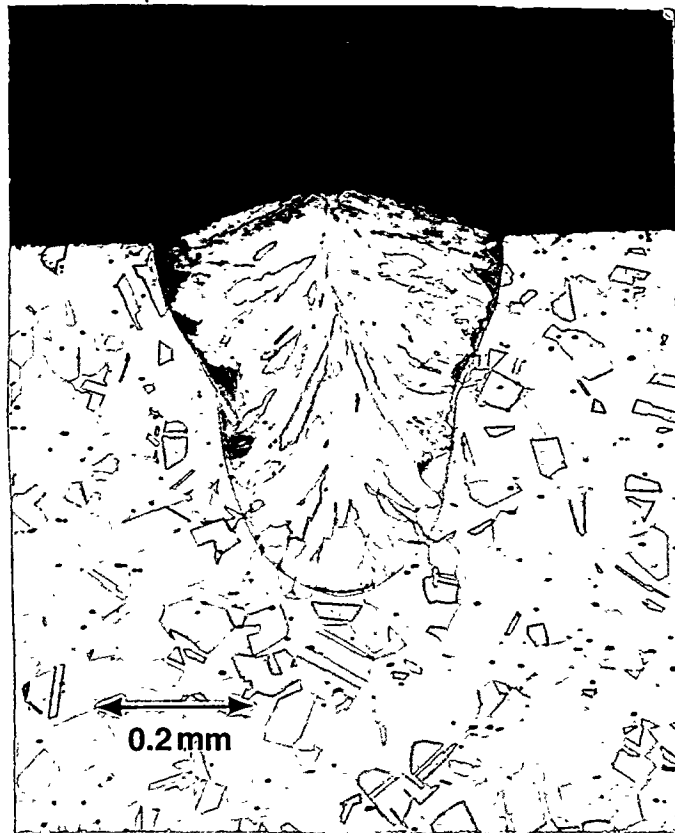


Fig. 2—Metallographic cross-section of CO₂ laser weld on 304SS indicating keyhole geometry. (930W, 212 mm/s, 9.1 MW/cm²)

DISCLAIMER

This report was prepared as an account of work sponsored by an agency of the United States Government. Neither the United States Government nor any agency thereof, nor any of their employees, makes any warranty, express or implied, or assumes any legal liability or responsibility for the accuracy, completeness, or usefulness of any information, apparatus, product, or process disclosed, or represents that its use would not infringe privately owned rights. Reference herein to any specific commercial product, process, or service by trade name, trademark, manufacturer, or otherwise does not necessarily constitute or imply its endorsement, recommendation, or favoring by the United States Government or any agency thereof. The views and opinions of authors expressed herein do not necessarily state or reflect those of the United States Government or any agency thereof.

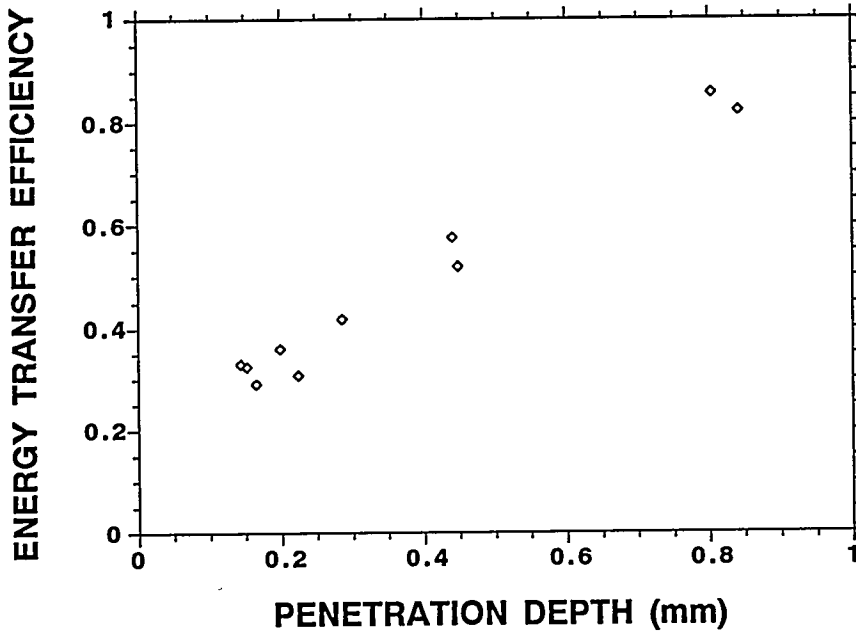


Fig. 3—Correlation between measured absorption and the depth of the fusion zone for 304 SS.

reflections is based on the premise that light rays will necessarily be reflected several times before exiting the weld cavity if the keyhole has a favorable geometry.

If we assume the cavity geometry to be a circular cone, then the incident laser rays will be reflected inside the cavity as is shown in Figure 4(a,b). Since for a triangle, any exterior angle is the sum of the two opposite interior angles, it can be seen in Figure 4(b) that the directional angle, θ_n , (or the external angle of triangle ABC) will increase by 2α at each reflection until the ray exits the cone. Given that the beam makes an angle ϕ to the perpendicular bisector of a right circular cone of angle 2α , then the calculation of the n th-directional angle θ_n proceeds as follows.

$$\begin{aligned} \theta_1 &= \phi + \alpha \\ \theta_2 &= \theta_1 + 2\alpha = \phi + \alpha + 2\alpha = \phi + 3\alpha \\ \theta_3 &= \theta_2 + 2\alpha = \phi + 3\alpha + 2\alpha = \phi + 5\alpha \\ \theta_n &= \theta_{n-1} + 2\alpha \end{aligned}$$

$$\text{therefore: } \theta_n = \phi + (2n-1)\alpha \quad [2]$$

where $(2n-1)$ is the usual way of representing a progression of odd integers. Equation [2] has been previously given by Eisenman and Bates (Ref. 6) for cone calorimeters. From [2] and the relation $\alpha = \tan^{-1}(r_k/d)$ where r_k is the radius of the cone or keyhole and d is the depth of penetration or the height of the cone, it can be shown that the number of reflections (n) for any ray is:

$$n = \frac{(\theta_n - \phi)}{2 \tan^{-1}(r_k/d)} + \frac{1}{2} \quad [3]$$

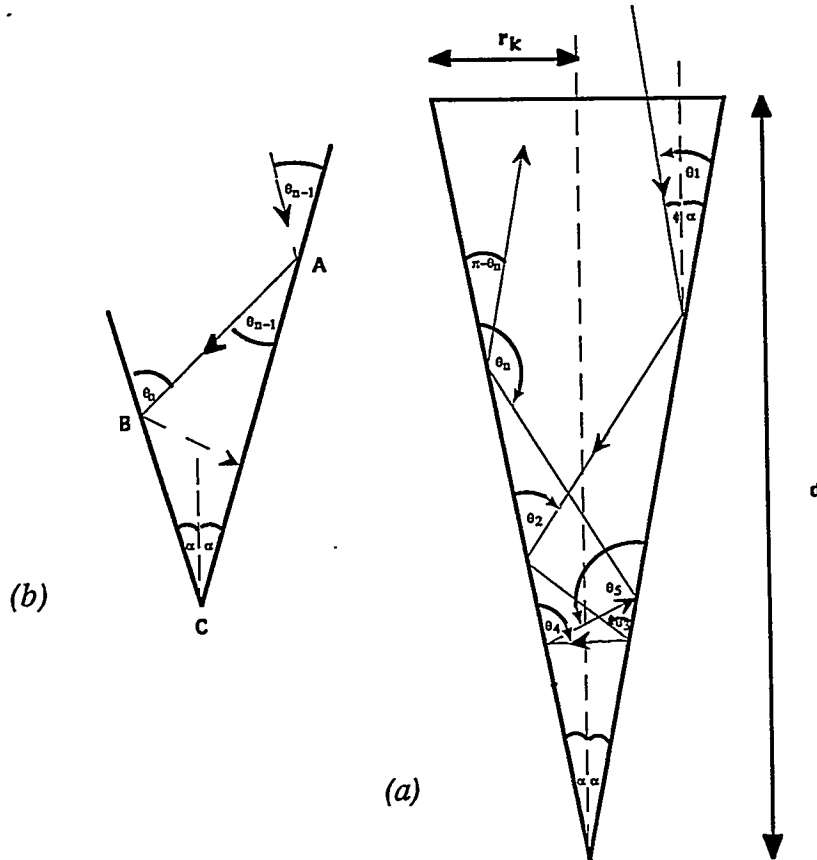


Fig. 4—(a) Relevance of cavity geometry to reflected light rays. (b) Geometric relationship between cone angle and a reflected ray.

The last reflection will occur when the light ray has changed direction and can no longer strike the walls of the cone. By similar triangles it can be seen that when $\pi - \theta_n$ is equal to the cone angle 2α , the light ray will exit parallel to the side of the cone. There are three cases to consider for θ_n (See figure 4).

- (i) $\theta_n < \pi - 2\alpha$ —reflection continues.
- (ii) $\theta_n = \pi - 2\alpha$ —beam exits cone parallel to the side of the cone.
- (iii) $\theta_n > \pi - 2\alpha$ —beam exits cone diverging from the side of the cone.

A special case for light ray exit is when $\theta_n = \pi - \alpha$, and $\phi=0$. This beam will exit the cone parallel to the axis and the incoming beam. This is the case first given by Mendenhall (Ref. 7) which results in the familiar expression:

$$n = \frac{\pi}{2\alpha} \quad [4]$$

The more general case for laser welding should include all rays that diverge from the side of the cone. Substituting (ii) and (iii) into [3] and solving for n gives:

$$n \geq \frac{(\pi - \phi)}{2 \tan^{-1}(r_k / d)} - \frac{1}{2} \quad [5]$$

To restrict the inequality to the correct positive integer values we must round the following expression to the next highest integer:

$$n = \frac{\pi - \phi}{2 \tan^{-1}(r_k / d)} - \frac{1}{2} \quad \text{or equivalently:} \quad n = \frac{\pi - \phi}{2\alpha} - \frac{1}{2} \quad [6]$$

One can see from [6] that for light rays that are not parallel to the axis of the cone (i.e. $\phi > 0$) the number of reflections will be somewhat reduced when compared with light rays that are more parallel. It is also obvious from [6] that for any light rays, more reflections will occur as the depth of penetration increases.

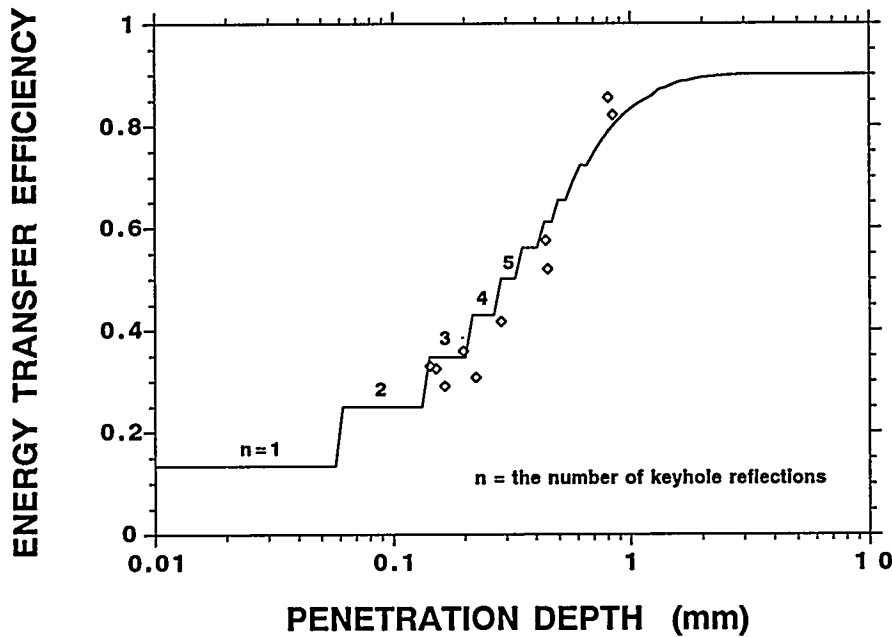


Fig. 5—Correlation of [9] with the experimental results for $R=0.85$ and $r_k=0.10$ mm

Laser beam absorption (A) in the weld pool depends on the liquid metal reflectivity (R) and the number of reflections in the weld pool cavity as follows:

$$A = 1 - R^n \quad [7]$$

The energy transferred to the part is equal to the laser energy absorbed minus radiative, convective, and vaporization losses to the surroundings. If we estimate these losses to be 10% of the absorbed laser energy (not to be confused with measurement losses discussed earlier) the following expression for energy transfer efficiency (η_t) is obtained:

$$\eta_t = 0.9(1 - R^n) \quad [8]$$

By combining equations [6] and [8], we obtain an expression for the relationship

between laser beam absorption and the keyhole dimensions r_k and d :

$$\eta_t = 0.9 \left[1 - R \left(\frac{\pi - \phi}{2 \tan^{-1}(r_k/d) - \frac{1}{2}} \right) \right] \quad [9]$$

If we assume that the laser light is roughly parallel to the depth of penetration, then $\phi=0$ and we can fit [9] to our data for penetration and energy transfer efficiency. Figure 5 shows the correlation between [9] and the experimental data. The value for liquid 304SS reflectivity used in the equation is 0.85 as given by Arata (Ref. 8).

Using this approach requires that the keyhole radius be assumed constant. Several fits of [9] to the data indicated that a keyhole radius of 0.10 mm would produce a good correlation. Since the focus spot radius for these welds is 0.059 mm, this size keyhole is reasonable. In addition, the resulting fusion zone surface widths varied from 0.21 mm to 0.66 mm in diameter. For the smallest welds this indicates that the keyhole size is close to the overall size of the weld but substantially less for the deep penetration welds.

Conclusions

1. It was found that the energy transfer efficiencies for CO₂ laser welds on 304 stainless steel varied from 0.29 to 0.86.
2. The energy transfer efficiency was found to decrease at high travel speeds and high irradiance where the weld penetration depth became as shallow as 0.13 mm.
3. Equations have been developed for the theory of multiple internal reflections, which correlate the keyhole cavity dimensions with the energy transfer efficiency.
4. The keyhole cavity radius for CO₂ laser welding of 304 stainless steel has been determined to be 0.1 mm for a focused laser beam with a spot radius of 0.059 mm.

Acknowledgments

The authors would like to acknowledge the exceptional technical support of Fred Hooper and Alice Kilgo. We would also like to thank Marcelino Essien for a careful review of the manuscript. This work was performed at Sandia National Laboratories, which is supported by the U.S. Department of Energy under contract number DE-AC04-94AL85000.

References

1. Huntington, C. A.; Eagar, T. W. 1983. Laser Welding of Aluminum and Aluminum Alloys. *Welding Journal* 62(4):105s-107s.
2. Kim, T. H.; Albright, C. E.; Chiang, S. 1990. The Energy Transfer Efficiency in Laser Welding Process. *Journal of Laser Applications* (Jan/Feb):23-28.
3. Fuerschbach, P. W. 1995. Measurement and Prediction of Energy Transfer Efficiency in Laser Beam Welding. *accepted for publication in Welding Journal*
4. Benzinger, T. H.; Kitzinger, C. 1949. Direct Calorimetry by Means of the Gradient Principle. *The Review of Scientific Instruments* 20(12):849-860.
5. Giedt, W. H.; Tallerico, L. N.; Fuerschbach, P. W. 1989. GTA Welding Efficiency: Calorimetric and Temperature Field Measurements. *Welding Journal* 68(1):28s-32s.
6. Eisenman, W. L.; Bates, R. L.; Merriam, J. D. 1963. Black Radiation Detector. *J. Opt. Soc. Am.* 53(6):729-734.
7. Mendenhall, C. E. 1911. On the Emissive Power of Wedge Shaped Cavities and their Use in Temperature Measurements. *The Astrophysical Journal* 33(2):91-97.
8. Arata, Y. 1986. *Plasma, Electron and Laser Beam Technology*; ASM: Metals Park, Ohio, p.237.